View metadata, citation and similar papers at core.ac.uk
brought to you by CORE
provided by University of Queensland eSpace

Novel Image Reconstruction Algorithm for a UWB Cylindrical Microwave Imaging System

Marek E. Bialkowski, Yifan Wang, Aslina Abu Bakar and Wee Chang Khor

School of ITEE, University of Queensland, St Lucia, Queensland, 4072, Australia
Email: {meb, yfwang, aslina, khor}@itee.uq.edu.au

***Abstract* — A theoretical and experimental study of a novel image reconstruction algorithm for an Ultra Wideband (UWB) Microwave Imaging System aiming at detecting and locating small targets in a homogenous circular cylindrical dielectric body is presented. The system uses a double circular scan in which the second scan is achieved after rotating by a small angle the antenna sub-system or the imaged body. The obtained two sets of data serve the purpose of subtracting the background that masks the target. Assuming that the target is asymmetric with respect to the axis of rotation, the difference data includes the original target and its negative "ghost". In order to eliminate the "ghost" only the positive valued difference data is extracted. This data is scaled and mapped to show the original target location. The validity of the proposed image reconstruction algorithm is demonstrated in an example of a cylindrical plastic container filled with a vegetable oil and small cylindrical targets.**

***Index Terms* —Microwave Imaging, Antennas, UWB, Radar.**

I. Introduction

Recent years have shown an increased interest in using active microwave techniques to obtain internal images of various objects. A particular focus has been on an application of these techniques to detect and locate a tumour within the woman's breast [1]. The principle of these techniques is that the healthy and cancerous tissues have considerably different dielectric properties in the microwave frequency region.

There have been two major approaches to see the inside of a dielectric body using microwaves. One approach employs so-called inverse scattering approach, in which the imaged body is surrounded by a number of microwave sensors operating at a single or multiple frequencies. By comparing the measured data by these sensors with the data produced from the solution of a forward full-wave EM problem, an image representing the distribution of a complex dielectric constant within the image body is produced. The regions having a large dielectric constant are identified as a target. The alternative is the ultra wideband (UWB) radar (mono or multi-static) approach in which the sensors transmit and receive short duration microwave pulses. In this case, the measured data is used to identify the locations producing an increased scatter within the image body. The two approaches have their own advantages and disadvantages. The inverse scattering approach does not require any *a priori* information about the imaged object to produce the complex dielectric constant distribution. However, in practice it requires large computational resources and often faces a difficulty to converge to the right solution due to an ill-conditioned non-linear problem. The UWB radar approach is approximate in nature and requires an estimate of average dielectric properties of the body to form an image. Its main challenge comes from a small return signal due to a target which is masked by a large magnitude signal caused by reflections at an air-imaged body interface.

In this paper the focus is on an ultra wideband radar technique for detecting and locating a small cylindrical object within a homogenous dielectric cylindrical body. We propose a new image reconstruction algorithm which uses the data obtained from two cylindrical scans. The first data is obtained from a uniform circular scan obtained either from an array antenna or a single antenna mechanically rotated around the imaged body. The other scan is obtained after rotating by a small angle the antenna scanning sub-system or the imaged body. The two sets of data serve the purpose of background (air-imaged body interface) subtraction. The difference data is suitably scaled and mapped to show the location of a large internal scatter. The proposed image reconstruction algorithm is demonstrated via full EM simulations and measurements.

The paper is organised as follows. Section II describes the configuration and principles of operation of a UWB microwave imaging system including the image reconstruction algorithm. Section III describes simulations and experiments verifying the validity of the proposed image reconstruction algorithm. Section IV concludes the paper.

II. Experimental Setup

Fig.1 shows configuration of the prototype UWB microwave imaging system. It includes a cylindrical scanning mechanical sub-system, a Vector Network Analyser (VNA) with time-domain processing capability, and an imaged body. The VNA transmits and receives short duration pulses using the step-frequency pulse synthesis technique described in [2]. The imaged object is a circular plastic container with a diameter of 125mm, thickness of 1mm and height of 100mm filled with canola oil with a relative permittivity, $_r$ of 3.5 to 4.2 and negligible losses, as measured with a dielectric coaxial probe in the frequency band from 2 to 12 GHz. The target is in the form of a small conducting circular cylinder placed vertically inside the container.

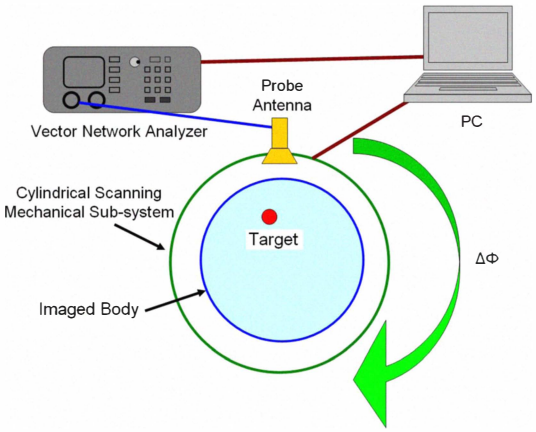

Fig. 1. Configuration of Microwave Imaging System

The probe antenna (sensor) is a UWB tapered slot antenna with corrugations. It is designed using a Finite Element Method design and analysis package, Ansoft HFSSv12. Fabricated on a Rogers RT6010LM substrate it features a compact size of 36mm × 36mm. Its photograph is shown in Fig.2.

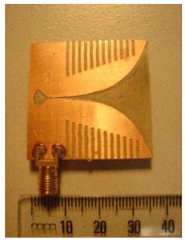

Fig. 2. Photograph of manufactured UWB Tapered Slot Antenna.

Its simulated and measured 10-dB return loss bandwidth is from 2.5 GHz to 11 GHz. Due to the use of corrugations, this antenna features an approximately constant directive radiation pattern with a narrow beam in the E-plane and a wide beam in the H-plane that helps to efficiently radiate power onto the imaged body across the entire UWB (3.1-10.6GHz). It is connected with a coaxial cable to the VNA. It is positioned vertically to produce vertical polarization. Depending on the choice of distance to the imaged container it produces different type of wavefront (planar, radial convex or radial concave) as the imaged body acts as a lens. In the first instance, the antenna is rotated around the container from 0° to 330° at an angular step equal to 30°. This movement emulates a 12-element uniform circular array antenna. When constructed, such a 12-element array offers a reasonable isolation between adjacent elements while providing a good spatial signal resolution on the circular periphery. In the next scan, the rotation starts at 15° degrees with the same step equal to 30° to cover the range of 15° to 345°. As a result, the two scans emulate a 24-element circular array with a 15° angular step.

Prior to measurements, the VNA is calibrated over UWB using a one-port (S11) calibration procedure [2]. At each antenna position, the VNA synthesizes a pulse using the time-domain capability of VNA. This procedure is repeated for all of the designated locations of the probe antenna. Following the data collection, a new image reconstruction procedure using the rotation/background subtraction concept is applied to see the inside of the container. The following steps make up this procedure:

1. Obtain twenty four (24) time-domain signals $\{S_i(t)\}$ i=1, 2, ..24 received by the antenna at angular positions $_i=(i-1)\times15°$.
2. Remove background by forming difference signals from adjacent antenna elements: $D_1(t)= S_2(t)-S_1(t)$, $D_2(t)= S_3(t)- S_2(t)$,... $D_{24}(t)= S_1(t)-S_{24}(t)$.
3. By extracting the positive-valued parts of signals $\{D_i(t)\}$, remove "ghost target" in $\{D_i(t)\}$ which was introduced in the "subtraction" step 2:

$$P_i(t)=\begin{cases} D_i(t) & \text{for } D_i(t)>0 \\ 0 & \text{for } D_i(t)<0 \end{cases}$$

4. Normalize $P_i(t)$ to compensate for the effect of radial spread or dielectric losses that are responsible for decay of the target signal with distance:
   $N_i(t)=P_i(t)/\max[P_i(t)]$
5. Estimate the relative dielectric constant ($_r$) and thus the propagation constant in the image body to achieve transformation of the obtained signals from the time-domain to the space-domain.
6. Depending on the obtained propagation constant and location of the antenna with respect to the image body, determine the type of wavefronts (planar or radial) formed inside the imaged body to estimate the time taken for the wave to strike the target and return to the antenna. This process is illustrated in Fig.3 where the wave incident on the target is planar and the wave scattered by the target is radial. For the shown geometry, the time taken by the signal to return to the antenna is given by $\tau = 2\{D + \sqrt{\varepsilon_r}(R + x)\}/c$ where c is the velocity of light and other symbols are explained in Fig.3.
7. Map the $N_i(\ )$ onto x_i=const using information from the previous step that the target is on the vertical line x_i=const in the imaged body.
8. Repeat step 7 for all signals $N_i(t)$, i=1,2,...12 using transformation from the local (x_i,y_i) to global (x_g,y_g) coordinate system.
9. Superimpose results for Ni(t) to get the image in the form of signal intensity and identify the target by the large image intensity.

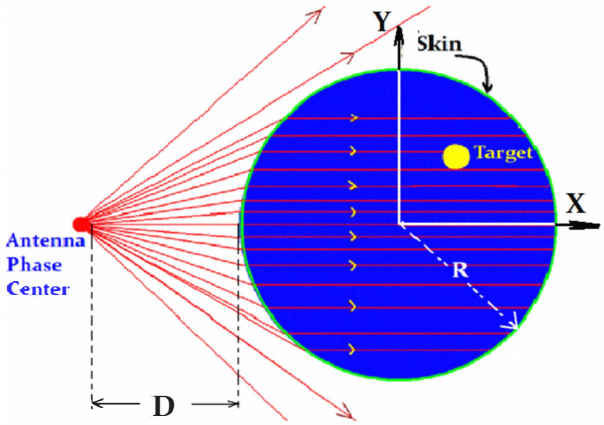

(a)

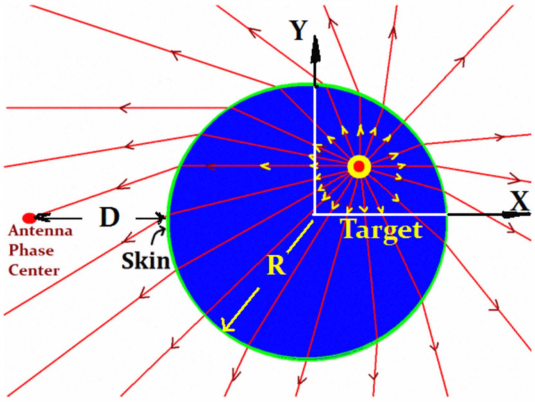

(b)

Fig. 3. Illustration of (a) wave incidence and (b) scattering.

At this stage it is worthwhile to point out the novelty of the proposed procedure. The presented image reconstruction procedure shows some relationship with the *confocal* microwave imaging algorithm proposed by E. Fear *et al.* [1]. Similarly as in [1], it is applicable to a cylindrical scanning system and thus is limited to the cases in which the target has no axial symmetry with respect to the cylindrical scanning system. For the axial location, the subtraction procedure leads to the target removal. If it is the case, the algorithm has to use the original data leading to the image showing both the background and the target. The differences between the new algorithm and that described in [1] concern both the background subtraction and data mapping. In [1], the acquired signals are averaged. This leads to smearing of the target location over a circular ring with the 1/N reduction factor (here N=12 or 24). The differences also concern the target signal compensation. In [1], the compensation factor responsible for the radial spread is used. As indicated in [1], this step may lead to emphasizing a clutter. Therefore, the compensation achieved by normalization outlined in step 4 of the proposed procedure seems to be a safer option.

III. Simulation and Experimental Results

Here we present simulation and experimental results for the proposed imaging algorithm for a 125mm diameter cylindrical container filled with canola oil and small cylindrical targets. Fig. 4 shows the simulation results obtained with CST Microwave Studio illustrating the effect of distance between the probe antenna and the imaged container on the resulting type of wavefront incident on the target.

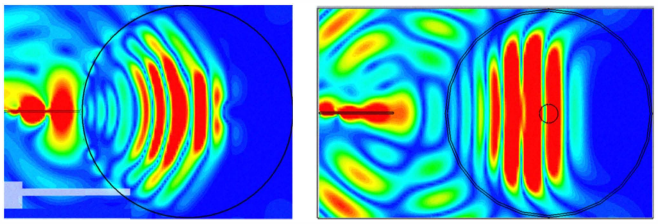

(a) (b)

Fig. 4. Different types of wavefronts as obtained from CST Microwave Office simulations: (a) radial (b) planar.

It can be observed from Fig.4 that depending on location of the antenna with respect to the imaged container ((a) 0mm and (b) 25mm), radial and planar wavefronts are formed. These different wavefronts influence the image reconstruction procedure. This problem has not been addressed in any earlier published works on UWB breast imaging techniques.

In order to assess the validity of the presented imaging algorithm, the comparison is made with a trivial algorithm assuming the presence and absence of the target. This is demonstrated using the data obtained from the time-domain CST Microwave Studio simulations. The antenna is assumed to be positioned at 25mm from the imaged container to achieve a planar wavefront incident on a target. Assuming that two sets of with and without the target from 12 probing antennas are available, the background image is removed by applying steps 3-7 of the proposed rotation/subtraction algorithm. The resulting image of a 15 mm diameter cylindrical target is presented in Fig.5.

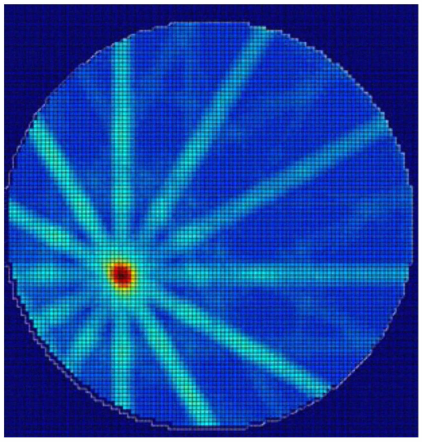

Fig. 5. Simulation imaging result of a 15mm diameter target located 25mm from the wall of the plastic container using the subtraction algorithm for data with and without the target.

The target is easily identified from the visual inspection of the produced image. However, the applied procedure with and without the target is not of much of practical importance. For example, when the breast is imaged the tumour is either present or absent. To overcome this shortfall, the proposed angular rotation and subtraction algorithm involving 24 antenna positions is applied when the target is present in the two phases of CST simulations. The imaging result is shown in Fig.6.

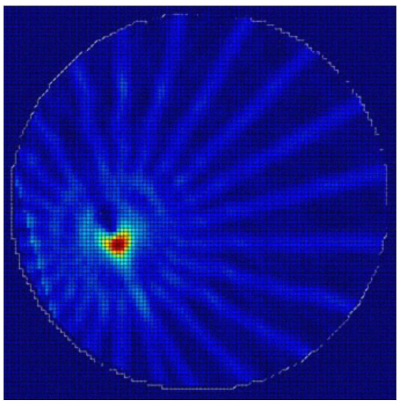

Fig. 6. Simulated imaging result of a 15mm diameter target located 25mm from the wall of the plastic container using the proposed image reconstruction algorithm.

The target's image presented in Fig.6 is similar in size and location to that in Fig.5. A small asymmetry is observed for the angle for which the target appears on the axis of symmetry of two adjacent antenna positions used in the subtraction process.

The final step includes an experimental verification of the proposed rotation and background subtraction imaging algorithm. Two experiments are undertaken. One is with a single target, as for Fig.6, and the other one is with an additional target of 4mm diameter. The measurements are performed in the 3.1-10.6 GHz band using the experimental setup of Fig. 1. Fig.7. shows the imaging result for a 15mm diameter target for a scenario similar to the one in Fig. 6.

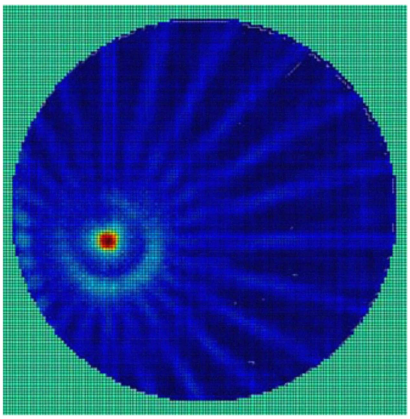

Fig. 7. Experimental imaging result of a 15mm diameter target located 25mm from the wall of the plastic container using the proposed image reconstruction algorithm.

By comparing the results of Fig. 7 with those of Fig. 6, it is apparent that the proposed rotation and subtraction algorithm works well both for the simulated and measured data.

The imaging result for two cylindrical targets one being 15mm and the other one of 4mm diameter are shown in Fig.8.

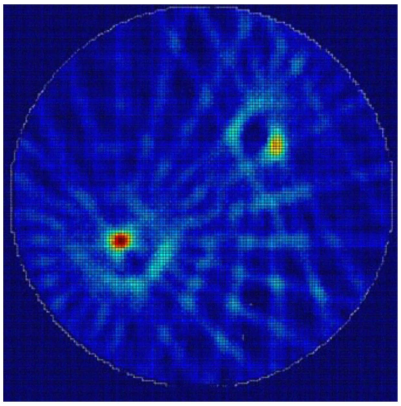

Fig. 8. Experimental imaging result of two cylindrical targets obtained using the proposed image reconstruction algorithm.

From results presented in Fig. 8 it is clear that the proposed imaging algorithm works well for multi-target scenarios.

IV. Conclusion

This paper has reported a novel image reconstruction algorithm for an Ultra Wideband (UWB) Microwave Imaging System to detect and locate small targets in a homogenous circular cylindrical body. The algorithm uses a difference of two signals obtained from adjacent antenna positions to remove background effect. The validity of the proposed algorithm has been verified both via full-wave EM simulations and experiment. Using the proposed algorithm, targets are detected just by visual inspection of the created image. The proposed algorithm should be of considerable interest to researchers working in the field of UWB microwave techniques for breast cancer detection as it overcomes the challenge in detecting of small internal targets masked by a large signal reflection at the air-imaged body interface.

Acknowledgment

The presented work has been supported by the Australian Research Council Discovery Grant DP1095746.

References

[1] E.C. Fear, S.C. Hagness, P.M. Meaney, M. Okoniewski and M.A. Stuchly, "Enhancing breast tumor detection with near-field imaging" *IEEE Microwave Magazine*, pp. 48-56, March 2002.

[2] M.E. Bialkowski, W.C. Khor and S. Crozier, "A planar microwave imaging system with step-frequency synthesized pulse using different calibration methods," Microwave and Optical Techn. Letters, vol. 48, No 3, pp. 511-516, 2006.